International Journal of Bridge Engineering (IJBE), Vol.8, No. 1, (2020), pp. 53-70

ANALYTICAL SOLUTIONS FOR THE FLEXURAL ANALYSIS OF ADVANCED COMPOSITE ARCHES

Atteshamuddin S. Sayyad[1] and Yuwaraj M. Ghugal[2]

[1,]Department of Civil Engineering, SRES's Sanjivani College of Engineering, Savitribai Phule Pune University, Kopargaon-423601, Maharashtra, India
[2]Department of Applied Mechanics, Government College of Engineering, Karad-415124, Maharashtra, India
e-mail: attu_sayyad@yahoo.co.in, ghugal@rediffmail.com

ABSTRACT: A great deal of literature is available on the flexural analysis of composite beams, plates and shells using higher order shear deformation theories. However, a limited research work is available on the flexural analysis of arches made up of functionally graded (FG) type composite materials using higher order theory. Therefore, flexural analysis of FG arches subjected to uniform load is the main focus of the present study. A trigonometric curved beam theory considering the effects of transverse shear and normal stresses is applied for the flexural analysis of two hinged FG arches. Material properties of FG arches are varied through the thickness according to the power-law distribution. The present theory imparts the sinusoidal variation of normal strain and cosine distribution of shear strain through the thickness. It satisfies the zero shear stress conditions on the top and bottom surfaces of the arch using constitutive relations. Equilibrium equations of the theory are derived within the framework of the principle of virtual work. Analytical solutions for the flexural analysis of two hinge arches are obtained using Navier's technique. The non-dimensional displacements and stresses are obtained for different radii of curvature and various values of power law coefficients. The results of present theory are compared with those of EBT, FSDT and PSDT theories. The numerical results presented in this study will be useful for the reference of future research in this area.

KEYWORDS: Bending; FG Arches; Normal Deformation; Shear Deformation; Trigonometric Beam Theory.

1 INTRODUCTION

Composite arches or curved beams subjected to static loading are widely appeared in highway as well as railway bridges and hence required accurate static flexural analysis i.e. accurate estimation of displacements and stresses in the composite arches subjected to transverse static loadings. Bernoulli-Euler

beam theory (EBT) [1] and Timoshenko beam theory (TBT) [2] also called as first order shear deformation theory (FSDT) predict inaccurate displacements and stresses in arches due to neglect of transverse shear and normal deformation effects. These effects are more pronounced in arches made up of advanced composite materials such as functionally graded (FG) materials. This has forced the researchers to develop the refined theories to account for the effect of transverse shear and normal deformations. All these higher-order theories are systematically documented by Sayyad and Ghugal [3-5]. One of the important and well-known higher order beam theories is the parabolic shear deformation theory of Reddy [6] which is widely used by many researchers.

Several articles have been published in the literature on static and free vibration analysis of laminated composite and sandwich curved beams using refined theories based on numerical methods. Some of them are presented by Bhimaraddi et al. [7], Qatu [8], Ecsedi and Dluhi [9], Marur and Kant [10], Guo et al. [11], Ye et al. [12], Thurnherr et al. [13], Eroglu [14], Kurtaran [15], Luu et al. [16], Nanda and Kapuria [17], Hajianmaleki and Qatu [18], Jun et al. [19], etc.

Functionally graded (FG) material is an advanced composite material in which elastic properties are varied continuously along the dimensions of the structure. FG materials possess a number of advantages in many engineering applications including bridges. In the last decade a lot of research has been carried out by researchers on analysis of beams, plates and shells made up of FG composite materials [20-42]. However, literature on static and free vibration analysis of FG arches is rarely available.

1.1 Novelty statements

This paper focuses on the analysis of FG arches subjected to uniform load and has the following novelties.

1) Many research papers have been published by researchers on the analysis of beams, plates and shells made up of FG composite materials in the last decade. However, a limited research work is available on analysis of arches/curved beams made up of FG composite material. Hence, static flexural analysis of FG arches is presented in this paper.
2) It is observed that the analysis of FG arches or curved beams considering the effect of transverse shear and normal deformations are also not available in the literature. Therefore, in the present study, a trigonometric curved beam theory considering the effects of both transverse shear and normal deformations is used for the analysis of FG arches.
3) Numerical results presented in this paper will be useful for the future researchers for the comparison of their results.

This paper includes six main sections. Section 1 deals with literature review and novelty statements. Section 2 represents geometry and material properties of the

arches. Sections 3 and 4 represent mathematical modeling and analytical solutions respectively. Numerical results along with discussion are presented in section 5 whereas section 6 represents important conclusions drawn from the study.

2 GEOMETRY AND MATERIAL PROPERTIES OF ARCHES

In the present study, advanced composite arches made up of FG composite material are considered in the mathematical formulation and numerical study. Geometry and coordinate systems of the arch under consideration are shown in Fig. 1. The arch has curved length L, cross-sectional area $b\times h$ and radius of curvature R. The beam occupies the region $0\leq x\leq L$; $-b/2\leq y\leq b/2$; $-h/2\leq z\leq h/2$ in Cartesian coordinate systems. The z-axis is assumed downward positive.

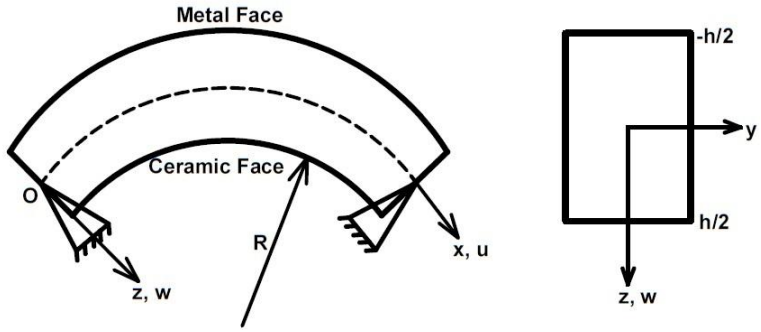

Figure 1. Two hinge arch under consideration

The FG composite material is made up from ceramic and metal. The elastic properties of material varied through the thickness of arch. The power-law is used for the gradation of elastic properties of the material. The law follows linear rule of mixture**.**

$$E(z)=E_m+(E_c-E_m)\left(\frac{1}{2}+\frac{z}{h}\right)^p \tag{1}$$

where $E(z)=E_m$ at $z=-h/2$ i.e. top surface and $E(z)=E_c$ at $z=h/2$ i.e. bottom surface; E_m and E_c represent the modulus of elasticity of metal and ceramic respectively; and p is the power-law coefficient. Eq. (1) leads to the variation of modulus of elasticity along the z-direction as shown in Fig. 2.

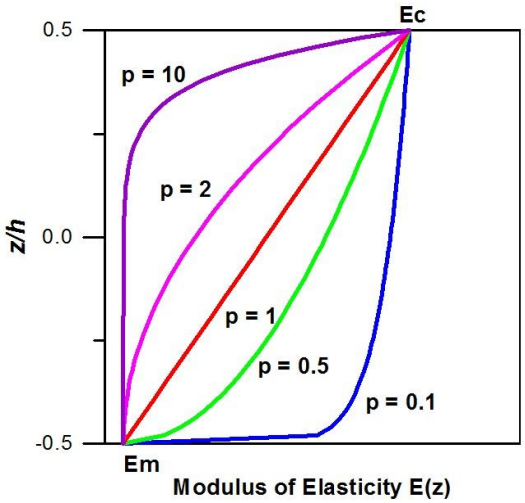

Figure 2. Gradation of modulus of elasticity across the thickness of FG arch

3 MATHEMATICAL MODELING

Mathematical modeling of the present trigonometric curved beam theory for FG arches is based on the following assumptions.

1) The displacement in *x*-direction (*u*) consists of the extension and bending components analogous to the classical curved beam theory, and shear component is considered to account the effect of shear deformation.
2) The curvature effect (arch) is incorporated by considering the radius of curvature in the displacement field as well as in strain calculations.
3) The transverse displacement consists of transverse normal strain effect (ε_z). Therefore, it is a function of two space variables (*x, z*).
4) The theory accounts for a traction free boundary condition at the top and bottom surfaces of the arch.
5) The two-dimensional Hooke's law is used to represent the state of stress at a point in arch.

Based on these assumptions, following displacement field is assumed for the present trigonometric curved beam theory,

$$u(x,z)=\left(1+\frac{z}{R}\right)u_0 - z\frac{\partial w_0}{\partial x}+\frac{h}{\pi}\sin\left(\frac{\pi z}{h}\right)\phi_x$$
$$w(x,z)=w_0+\cos\left(\frac{\pi z}{h}\right)\phi_z \qquad (2)$$

where *u* and *w* are the displacements in *x*- and *z*-directions, respectively; u_0 and w_0 are the displacements of neutral axis in *x*- and *z*- directions,

respectively; R is the radius of curvature; ϕ_x and ϕ_z are the unknown functions associated with transverse shear and normal deformations. Trigonometric sine and cosine functions are assumed according to transverse shearing strain distribution across the thickness of the arch. All four unknown variables $(u_0, w_0, \phi_x, \phi_z)$ are the functions of variable x. The nonzero normal strains corresponding to the present displacement field are given as;

$$\begin{Bmatrix} \varepsilon_x \\ \varepsilon_z \\ \gamma_{xz} \end{Bmatrix} = \begin{Bmatrix} \dfrac{\partial u_0}{\partial x} - z\dfrac{\partial^2 w_0}{\partial x^2} + \dfrac{h}{\pi}\sin\left(\dfrac{\pi z}{h}\right)\dfrac{\partial \phi_x}{\partial x} + \dfrac{w_0}{R} + \cos\left(\dfrac{\pi z}{h}\right)\dfrac{\phi_z}{R} \\ -\dfrac{\pi}{h}\sin\left(\dfrac{\pi z}{h}\right)\phi_z \\ \cos\left(\dfrac{\pi z}{h}\right)\left[\phi_x + \dfrac{\partial \phi_z}{\partial x}\right] \end{Bmatrix} \tag{3}$$

The arch is made up of FG composite materials where modulus of elasticity is varying through the thickness i.e. z-direction. Therefore, stiffness coefficients (Q_{ij}) are functions of z. The generalized Hooke's law is used to obtain stresses $(\sigma_x, \sigma_z, \tau_{xz})$ in FG arches as

$$\begin{Bmatrix} \sigma_x \\ \sigma_z \\ \tau_{xz} \end{Bmatrix} = \begin{bmatrix} Q_{11}(z) & Q_{12}(z) & 0 \\ Q_{12}(z) & Q_{22}(z) & 0 \\ 0 & 0 & Q_{33}(z) \end{bmatrix} \begin{Bmatrix} \varepsilon_x \\ \varepsilon_z \\ \gamma_{xz} \end{Bmatrix} \tag{4}$$

where Q_{ij} are the stiffness coefficients correlated with the engineering constants as follows:

$$Q_{11}(z) = Q_{22}(z) = \frac{E(z)}{1-\mu^2}, \quad Q_{12}(z) = \frac{\mu E(z)}{1-\mu^2} \quad \text{and} \quad Q_{33}(z) = \frac{E(z)}{2(1+\mu)} \tag{5}$$

Governing equations of the present trigonometric curved beam theory are derived by using the principle of virtual work as stated below:

$$b\int_0^L \int_{-h/2}^{h/2} \left(\sigma_x \delta\varepsilon_x + \sigma_z \delta\varepsilon_z + \tau_{xz} \delta\gamma_{xz}\right) dz\, dx - \int_0^L q(x)\delta w\, dx = 0 \tag{6}$$

Substitution of strain and stress expressions from Eqs. (3) and (4) into Eq. (6), one can get the following expression.

$$\int_0^L \begin{pmatrix} N_x \dfrac{\partial \delta u_0}{\partial x} - M_x^c \dfrac{\partial^2 \delta w_0}{\partial x^2} + M_x^s \dfrac{\partial \delta \phi_x}{\partial x} + N_x \dfrac{\delta w_0}{R} \\ + Q_z \dfrac{\delta \phi_z}{R} + Q_{zz}\, \delta\phi_z + V_z\, \delta\phi_x + V_z \dfrac{\partial \delta \phi_z}{\partial x} - q(x)\delta w \end{pmatrix} dx = 0 \tag{7}$$

After integrating Eq. (7) by parts, one can get the following equation

$$\left[N_x\delta u_0\big|_0^L-\int_0^L\frac{\partial N_x}{\partial x}\delta u_0dx\right]-\left[M_x^c\frac{d\delta w_0}{dx}\bigg|_0^L-\frac{dM_x^c}{dx}\delta w_0\bigg|_0^L+\int_0^L\frac{d^2M_x^c}{dx^2}\delta w_0dx\right]$$
$$+\left[M_x^s\delta\phi_x\big|_0^L-\int_0^L\frac{dM_x^s}{dx}\delta\phi_xdx\right]+N_x\frac{\delta w_0}{R}+Q_z\frac{\delta\phi_z}{R}+Q_{zz}\delta\phi_z+V_z\delta\phi_x$$
$$+\left[V_z\delta\phi_z\big|_0^L-\int_0^L\frac{dV_z}{dx}\delta\phi_zdx\right]-q(x)\left[\delta w_0+\cos\left(\frac{\pi z}{h}\right)\delta\phi_z\right]=0 \tag{8}$$

where $\left(N_x,M_x^c,M_x^s,Q_z,Q_{zz},V_z\right)$ are the force and moment resultants associated with the present trigonometric curved beam theory as defined below:

$$N_x=\int_{-h/2}^{+h/2}\sigma_x\,dz,\quad M_x^c=\int_{-h/2}^{+h/2}\sigma_x\,z\,dz,$$
$$M_x^s=\int_{-h/2}^{+h/2}\sigma_x\frac{h}{\pi}\sin\left(\frac{\pi z}{h}\right)dz,\quad Q_z=\int_{-h/2}^{+h/2}\sigma_x\cos\left(\frac{\pi z}{h}\right)dz, \tag{9}$$
$$Q_{zz}=-\int_{-h/2}^{+h/2}\sigma_z\frac{\pi}{h}\sin\left(\frac{\pi z}{h}\right)dz,\quad V_z=\int_{-h/2}^{+h/2}\tau_{xz}\cos\left(\frac{\pi z}{h}\right)dz$$

Substituting expressions of stresses in Eq. (9), the following expressions for the stress resultants (force and moments) in terms of displacement variables (u_0,w_0,ϕ_x,ϕ_z) can be obtained.

$$\begin{aligned}
N_x&=A_{11}\frac{\partial u_0}{\partial x}-B_{11}\frac{\partial^2w_0}{\partial x^2}+B_{11}^s\frac{\partial\phi_x}{\partial x}+A_{11}\frac{w_0}{R}+D_{11}\frac{\phi_z}{R}+E_{12}\phi_z\\
M_x^c&=B_{11}\frac{\partial u_0}{\partial x}-F_{11}\frac{\partial^2w_0}{\partial x^2}+F_{11}^s\frac{\partial\phi_x}{\partial x}+B_{11}\frac{w_0}{R}+D_{11}^s\frac{\phi_z}{R}+E_{12}^s\phi_z\\
M_x^s&=B_{11}^s\frac{\partial u_0}{\partial x}-F_{11}^s\frac{\partial^2w_0}{\partial x^2}+G_{11}^s\frac{\partial\phi_x}{\partial x}+B_{11}^s\frac{w_0}{R}+H_{11}^s\frac{\phi_z}{R}+J_{12}^s\phi_z\\
Q_z&=D_{11}\frac{\partial u_0}{\partial x}-D_{11}^s\frac{\partial^2w_0}{\partial x^2}+H_{11}^s\frac{\partial\phi_x}{\partial x}+D_{11}\frac{w_0}{R}+K_{11}^s\frac{\phi_z}{R}+L_{12}^s\phi_z\\
Q_{zz}&=E_{12}\frac{\partial u_0}{\partial x}-E_{12}^s\frac{\partial^2w_0}{\partial x^2}+J_{12}^s\frac{\partial\phi_x}{\partial x}+E_{12}\frac{w_0}{R}+L_{12}^s\frac{\phi_z}{R}+L_{22}^s\phi_z\\
V_z&=K_{33}^s\left(\phi_x+\frac{\partial\phi_z}{\partial x}\right)
\end{aligned} \tag{10}$$

where the extensional, bending and coupling stiffness coefficients appeared in the Eq. (10) are as follows:

$$A_{11}=b\int_{-h/2}^{h/2} C_{11}(z)\,dz,\;\; B_{11}=b\int_{-h/2}^{h/2} C_{11}(z)\,z\,dz,\; F_{11}=b\int_{-h/2}^{h/2} C_{11}(z)\,z^2\,dz,$$

$$F_{11}^s=b\int_{-h/2}^{h/2} C_{11}(z)\,z\frac{h}{\pi}\sin\left(\frac{\pi z}{h}\right)dz,\; B_{11}^s=b\int_{-h/2}^{h/2} C_{11}(z)\frac{h}{\pi}\sin\left(\frac{\pi z}{h}\right)dz,$$

$$D_{11}=b\int_{-h/2}^{h/2} C_{11}(z)\cos\left(\frac{\pi z}{h}\right)dz,\; D_{11}^s=b\int_{-h/2}^{h/2} C_{11}(z)\,z\cos\left(\frac{\pi z}{h}\right)dz,$$

$$E_{12}=-b\int_{-h/2}^{h/2} C_{12}(z)\frac{\pi}{h}\sin\left(\frac{\pi z}{h}\right)dz,$$

$$E_{12}^s=-b\int_{-h/2}^{h/2} C_{12}(z)\,z\frac{\pi}{h}\sin\left(\frac{\pi z}{h}\right)dz,\; G_{11}^s=b\int_{-h/2}^{h/2} C_{11}(z)\left[\frac{h}{\pi}\sin\left(\frac{\pi z}{h}\right)\right]^2 dz,$$

$$H_{11}^s=b\int_{-h/2}^{h/2} C_{11}(z)\frac{h}{\pi}\sin\left(\frac{\pi z}{h}\right)\cos\left(\frac{\pi z}{h}\right)dz,$$

$$J_{12}^s=-b\int_{-h/2}^{h/2} C_{12}(z)\left[\frac{h}{\pi}\sin\left(\frac{\pi z}{h}\right)\right]^2 dz,\; E_{12}^s=-b\int_{-h/2}^{h/2} C_{12}(z)\,z\frac{\pi}{h}\sin\left(\frac{\pi z}{h}\right)dz,$$

$$L_{12}^s=-b\int_{-h/2}^{h/2} C_{12}(z)\cos\left(\frac{\pi z}{h}\right)\frac{\pi}{h}\sin\left(\frac{\pi z}{h}\right)dz,$$

$$L_{22}^s=b\int_{-h/2}^{h/2} C_{22}(z)\left[\frac{\pi}{h}\sin\left(\frac{\pi z}{h}\right)\right]^2 dz,$$

$$K_{11}^s=b\int_{-h/2}^{h/2} C_{11}(z)\left[\cos\left(\frac{\pi z}{h}\right)\right]^2 dz,\; K_{33}^s=b\int_{-h/2}^{h/2} C_{33}(z)\left[\cos\left(\frac{\pi z}{h}\right)\right]^2 dz, \tag{11}$$

Governing equations associated with the present trigonometric curved beam theory are obtained by collecting the coefficients of displacement variables ($\delta u_0, \delta w_0, \delta\phi_x, \delta\phi_z$) from Eq. (8) and setting them equal to zero.

$$\begin{aligned}
\delta u_0 :&\quad \frac{\partial N_x}{\partial x}=0\\
\delta w_0 :&\quad \frac{\partial^2 M_x^c}{\partial x^2}-\frac{N_x}{R}+q(x)=0\\
\delta\phi_x :&\quad \frac{\partial M_x^s}{\partial x}-V_z=0\\
\delta\phi_z :&\quad \frac{\partial V_z}{\partial x}-Q_{zz}-\frac{Q_z}{R}+q(x)\cos\left(\frac{\pi z}{h}\right)=0
\end{aligned} \tag{12}$$

The boundary terms in the Eq. (8) represent the boundary conditions. Following are the boundary conditions for arches associated with the present trigonometric curved beam theory.

$$\begin{aligned} N_x = 0 \quad & \text{or} \quad u_0 = 0 \\ M_x^c = 0 \quad & \text{or} \quad \frac{\partial w_0}{\partial x} = 0 \\ \partial M_x^c / \partial x = 0 \quad & \text{or} \quad w_0 = 0 \\ M_x^s = 0 \quad & \text{or} \quad \phi_x = 0 \\ V_z = 0 \quad & \text{or} \quad \phi_z = 0 \end{aligned} \tag{13}$$

By substituting the force and moment resultants from Eq. (10) into Eq. (12), the governing equations can be expressed in displacement variables as follows:

$$\begin{aligned} \delta u_0 : & A_{11}\frac{\partial^2 u_0}{\partial x^2} - B_{11}\frac{\partial^3 w_0}{\partial x^3} + \frac{A_{11}}{R}\frac{\partial w_0}{\partial x} + B_{11}^s\frac{\partial^2 \phi_x}{\partial x^2} + \left(\frac{D_{11}}{R} + E_{12}\right)\frac{\partial \phi_z}{\partial x} = 0 \\ \delta w_0 : & B_{11}\frac{\partial^3 u_0}{\partial x^3} - \frac{A_{11}}{R}\frac{\partial u_0}{\partial x} - F_{11}\frac{\partial^4 w_0}{\partial x^4} + \frac{2B_{11}}{R}\frac{\partial^2 w_0}{\partial x^2} - \frac{A_{11}}{R^2}w_0 + F_{11}^s\frac{\partial^3 \phi_x}{\partial x^3} \\ & - \frac{B_{11}^s}{R}\frac{\partial \phi_x}{\partial x} + \left(\frac{D_{11}^s}{R} + E_{12}^s\right)\frac{\partial^2 \phi_z}{\partial x^2} - \left(\frac{D_{11}}{R^2} + \frac{E_{12}}{R}\right)\phi_z + q = 0 \\ \delta \phi_x : & B_{11}^s\frac{\partial^2 u_0}{\partial x^2} - F_{11}^s\frac{\partial^3 w_0}{\partial x^3} + \frac{B_{11}^s}{R}\frac{\partial w_0}{\partial x} + G_{11}^s\frac{\partial^2 \phi_x}{\partial x^2} \\ & - K_{33}^s\phi_x + \left(\frac{H_{11}^s}{R} + J_{12}^s - K_{33}^s\right)\frac{\partial \phi_z}{\partial x} = 0 \\ \delta \phi_z : & -\left(\frac{D_{11}}{R} + E_{12}\right)\frac{\partial u_0}{\partial x} + \left(\frac{D_{11}^s}{R} + E_{12}^s\right)\frac{\partial^2 w_0}{\partial x^2} - \left(\frac{D_{11}}{R^2} + \frac{E_{12}}{R}\right)w_0 \\ & - \left(\frac{H_{11}^s}{R} + J_{12}^s - K_{33}^s\right)\frac{\partial \phi_x}{\partial x} + K_{33}^s\frac{\partial^2 \phi_z}{\partial x^2} - \left(\frac{2L_{12}^s}{R} + \frac{K_{11}^s}{R^2} + L_{22}^s\right)\phi_z = 0 \end{aligned} \tag{14}$$

Eqs. (14) are the governing equations for advanced composite arches made up of functionally graded composite materials.

4 ANALYTICAL SOLUTIONS FOR TWO HINGE ARCHES

The Navier's technique is used for obtaining analytical solutions for the static flexural analysis of two hinge arches under uniform loading**.** The arch has following boundary conditions at ends.

$$w_0 = N_x = M_x^c = M_x^s = 0 \quad \text{at } x = 0 \text{ and } x = L \tag{15}$$

The unknown variables u_0, w_0, ϕ_x, ϕ_z in the displacement field are expanded in trigonometric series which satisfy the boundary conditions mentioned in Eq. (15).

$$\{u_0, \phi_x\} = \sum_{m=1,3,5}^{\infty} (u_m, \phi_{xm}) \cos\left(\frac{m\pi x}{L}\right)$$

$$\{w_0, \phi_z\} = \sum_{m=1,3,5}^{\infty} (w_m, \phi_{zm}) \sin\left(\frac{m\pi x}{L}\right) \tag{16}$$

$$q(x) = \sum_{m=1,3,5}^{\infty} \frac{4q_0}{m\pi} \sin\left(\frac{m\pi x}{L}\right)$$

where $(u_m, w_m, \phi_{xm}, \phi_{zm})$ are the unknown coefficients and q_0 is the maximum intensity of the uniform load. Substitution of Eq. (16) into the Eqs. (14) leads to a set of algebraic equations which can be written in the following matrix form

$$[K]\{\Delta\} = \{F\} \tag{17}$$

where elements of stiffness matrix [*K*], displacement vector $\{\Delta\}$ and force vector **{***F***}** are as follows:

$$\begin{gathered}
K_{11} = -A_{11}\,\alpha^2, \quad K_{12} = \left(B_{11}\alpha^3 + \frac{A_{11}}{R}\alpha\right), \quad K_{13} = -B^s_{11}\alpha^2, \\
K_{14} = \left(\frac{D_{11}}{R} + E_{12}\right)\alpha, K_{22} = \left(-F_{11}\,\alpha^4 - \frac{2B_{11}}{R}\alpha^2 - \frac{A_{11}}{R^2}\right), \\
K_{23} = \left(F^s_{11}\alpha^3 + \frac{B^s_{11}}{R}\alpha\right), \\
K_{24} = \left(-E^s_{12}\alpha^2 - \frac{D^s_{11}}{R}\alpha^2 - \frac{D_{11}}{R^2} - \frac{E_{12}}{R}\right), \quad K_{33} = \left(-G^s_{11}\alpha^2 - K^s_{33}\right), \\
K_{34} = \left(\frac{H^s_{11}}{R} + J^s_{12} - K^s_{33}\right)\alpha, \quad K_{44} = \left(-K^s_{33}\alpha^2 - \frac{K^s_{11}}{R^2} - \frac{2L^s_{12}}{R} - L^s_{22}\right), \\
\{\Delta\} = \{u_m, w_m, \phi_{xm}, \phi_{zm}\}^T \quad \text{and} \quad \{F\} = \left\{0, \frac{4q_0}{m\pi}, 0, 0\right\}^T
\end{gathered} \tag{18}$$

Stiffness matrix is always symmetric matrix. Solution of Eq. (17) gives values of unknown coefficients of Eq. (16). Using these values displacement variables of Eq. (2) can be determined. With the help of displacement variables, one can determine displacements and stresses in two hinge arches subjected to uniform load.

5 NUMERICAL RESULTS AND DISCUSSION

The present trigonometric curved beam theory is applied for the flexural analysis of FG composite arches subjected to uniform load. The arch is made up of ceramic (Al_2O_3: E_c = 380 GPa, μ_c = 0.3) and metal (Al: E_m = 70 GPa, μ_m =

0.3). The numerical results are presented in the following non-dimensional form.

$$\bar{u}\left(x=0,\ z=-h/2\right)=\frac{100\,u\,E_m\,h^3}{q_0L^4},$$
$$\bar{w}\left(x=L/2,\ z=0\right)=\frac{100\,w\,E_m\,h^3}{q_0L^4},$$
$$\bar{\sigma}_x\left(x=L/2,\ z=-h/2\right)=\frac{\sigma_x\,h}{q_0L}, \tag{19}$$
$$\bar{\tau}_{xz}\left(x=0,\ z=0\right)=\frac{\tau_{xz}\,h}{q_0L}$$

Convergence of the numerical results is found at m = 11 for the transverse displacement and m = 25 for the axial displacement and stresses. The length of the beam is taken as 1m (L = 1m) for all problems. Thickness and radius of curvature are varying according to L/h and R/L ratios.

The numerical results of displacements and stresses are presented in Tables 1 through 6 and plotted graphically in Figs. 3 through 8. The thickness of arch is taken as ***h.*** To compare the displacements and stresses obtained by the present theory, those are also obtained using parabolic shear deformation theory (PSDT) of Reddy [6], first order shear deformation theory (FSDT) of Timoshenko [2] and Euler-Bernoulli beam theory (EBT) [1]. The PSDT, FSDT and EBT neglected effects of transverse normal stress (σ_z).

Table 1 shows a comparison of transverse displacement obtained for FG composite arches subjected to uniform load. Numerical results are presented for aspect ratio (L/h) = 5, different values of radius of curvature to length (R/L= 5,10,20,50,100) ratio and different values of power-law coefficient (p = 0,1,2,5,10). From Table 1 it is pointed out that the present theory underestimates the transverse displacement compared to those obtained by using PSDT for all values of R/L. The EBT shows significant difference in the displacements due to neglect of transverse shear and normal strains. The values of non-dimensional transverse displacement increase with an increase in power law coefficients; because, increase in the power-law coefficients increases the flexibility of arches. Fig. 3 shows through-the-thickness distribution of transverse displacement. Due to transverse normal deformation effect, the value of transverse displacement is not constant through the thickness. Table 2 and Fig. 4 show the variation of transverse displacement along the length (x/L). Fig. 4 satisfies the boundary conditions, i.e. zero at supports (x = 0 and x = L) and maximum at the center of length (x=L/2).

Table 3 shows a comparison of axial stress of FG arches subjected to uniform load. Maximum values of axial stress are obtained at m = 25, L/h = 5, p =

(0,1,2,5,10) and *R/L* = (5,10,20,50,100). EBT, FSDT underestimate the axial stress for all values of power law coefficients and *R/L* ratios. Axial stress increases with increase in power law coefficient as well as *R/L* ratio. Fig. 5 shows through-the-thickness distributions of axial stress in FG arches subjected to uniform load. It is pointed out that the axial stress is zero at $z/h = 0$ for $p = 0$, however, for non-zero value of p (=1,2,5,10…) axial stress is not zero at $z/h = 0$. This is due to gradation of material properties across the thickness. In Fig. 5, $z/h = -0.5$ to $z/h = 0$ represent a compression zone, whereas $z/h = 0$ to $z/h = 0.5$ represents a tension zone. It is also observed that axial stress in tension zone increases with an increase in power law coefficient. Table 4 shows variation of axial stress along the length of the arch. Also depicted graphically in Fig. 6. Axial stress is maximum at the center and zero at the support.

Table 5 shows comparison of transverse shear stress obtained using the present theory and PSDT. EBT predicts zero value of transverse shear stress due to neglect of transverse shear deformation. Examination of Table 5 reveals that the effect of curvature on shear stress is negligible. For all values of *R/L* ratio, shear stress is almost same. Fig. 7 shows through-the-thickness distribution of transverse shear stress, which reveals that the maximum shear stress is not at z/h = 0 for p = 1,2,5,10. This is due to gradation of elastic properties of FG material. Table 6 and Fig. 8 show the variation of transverse shear stress along the length satisfying boundary conditions, i.e. maximum at supports and zero at center of the span.

Table 1. Comparison of the transverse displacements of FG arches under uniform load (*L/h*=5)

Theory	*p*	*R/L*=5	*R/L*=10	*R/L*=20	*R/L*=50	*R/L*=100	*R/L*=∞ (Beam)
Present	0	3.1355	3.1356	3.1357	3.1357	3.1357	3.1357
Bernoulli-Euler [1]		2.8781	2.8782	2.8783	2.8783	2.8783	2.8783
Timoshenko [2]		3.1654	3.1656	3.1657	3.1657	3.1657	3.1657
Reddy [6]		3.1651	3.1653	3.1654	3.1654	3.1654	3.1654
Present	1	6.1482	6.1316	6.1233	6.1184	6.1168	6.1151
Bernoulli-Euler [1]		5.7861	5.7704	5.7626	5.7580	5.7565	5.7746
Timoshenko [2]		6.2933	6.2763	6.2678	6.2628	6.2612	6.2599
Reddy [6]		6.2896	6.2726	6.2641	6.2591	6.2575	6.2594
Present	2	7.8773	7.8558	7.8453	7.8389	7.8368	7.8347
Bernoulli-Euler [1]		7.4440	7.4237	7.4138	7.4078	7.4058	7.4003
Timoshenko [2]		8.0821	8.0601	8.0493	8.0427	8.0406	8.0303
Reddy [6]		8.1136	8.0915	8.0807	8.0741	8.0719	8.0677
Present	5	9.6298	9.6069	9.5956	9.5889	9.5866	9.5844
Bernoulli-Euler [1]		8.8016	8.7807	8.7704	8.7643	8.7622	8.7508
Timoshenko [2]		9.7434	9.7203	9.7088	9.7020	9.6997	9.6483
Reddy [6]		9.8705	9.8471	9.8355	9.8286	9.8263	9.8291
Present	10	10.787	10.761	10.748	10.740	10.738	10.735
Bernoulli-Euler [1]		9.6544	9.6311	9.6195	9.6123	9.6105	9.6072
Timoshenko [2]		10.776	10.750	10.737	10.729	10.727	10.719
Reddy [6]		10.992	10.965	10.952	10.944	10.942	10.938

Table 2. Transverse displacement for various values of length coordinate (x/L)

Theory	p	x/L=0	x/L=0.2	x/L=0.4	x/L=0.5	x/L=0.6	x/L=0.8	x/L=1
Present	0	0	1.8738	2.9879	3.1355	2.9879	1.8738	0
Present	1	0	3.6723	5.8593	6.1482	5.8593	3.6723	0
Present	2	0	4.7075	7.5075	7.8773	7.5075	4.7075	0
Present	5	0	5.7668	9.1797	9.6298	9.1797	5.7668	0
Present	10	0	6.4651	10.2842	10.787	10.2842	6.4651	0

Table 3. Comparison of the axial stress of FG arches under uniform load (L/h=5)

Theory	p	R/L=5	R/L=10	R/L=20	R/L=50	R/L=100	R/L=∞ (Beam)
Present	0	3.8220	3.8401	3.8491	3.8545	3.8563	3.8581
Bernoulli-Euler [1]		3.7150	3.7326	3.7413	3.7466	3.7483	3.7500
Timoshenko [2]		3.7150	3.7326	3.7413	3.7466	3.7483	3.7500
Reddy [6]		3.7647	3.7825	3.7914	3.7967	3.7985	3.8020
Present	1	5.9366	5.9583	5.9689	5.975	5.9771	5.9791
Bernoulli-Euler [1]		5.7526	5.7736	5.7839	5.7898	5.7918	5.7959
Timoshenko [2]		5.7526	5.7736	5.7839	5.7898	5.7918	5.7959
Reddy [6]		5.8416	5.8630	5.8734	5.8794	5.8815	5.8836
Present	2	6.9448	6.9679	6.9791	6.9856	6.9877	6.9899
Bernoulli-Euler [1]		6.7226	6.7449	6.7558	6.7621	6.7641	6.7676
Timoshenko [2]		6.7226	6.7449	6.7558	6.7621	6.7641	6.7676
Reddy [6]		6.8337	6.8564	6.8674	6.8738	6.8759	6.8826
Present	5	8.1850	8.2117	8.2246	8.2321	8.2346	8.2371
Bernoulli-Euler [1]		7.8903	7.9161	7.9285	7.9357	7.9382	7.9428
Timoshenko [2]		7.8903	7.9161	7.9285	7.9357	7.9382	7.9428
Reddy [6]		8.0540	8.0803	8.0930	8.1004	8.1028	8.1106
Present	10	9.7885	9.8207	9.8362	9.8454	9.8485	9.8515
Bernoulli-Euler [1]		9.4459	9.4770	9.4919	9.5008	9.5038	9.5228
Timoshenko [2]		9.4459	9.4770	9.4919	9.5008	9.5038	9.5228
Reddy [6]		9.6378	9.6695	9.6847	9.6938	9.6968	9.7122

Table 4. Axial stress for various values of length coordinate (x/L)

Theory	p	x/L=0	x/L=0.2	x/L=0.4	x/L=0.5	x/L=0.6	x/L=0.8	x/L=1
Present	0	0	2.4662	3.6699	3.8220	3.6699	2.4662	0
Present	1	0	3.8324	5.7003	5.9366	5.7003	3.8324	0
Present	2	0	4.4888	6.6691	6.9448	6.6691	4.4888	0
Present	5	0	5.3050	7.8617	8.1850	7.8617	5.3050	0
Present	10	0	6.3396	9.4017	9.7885	9.4017	6.3396	0

Table 5. Comparison of the transverse shear stress of FG arches under uniform load (L/h=5)

Theory	p	R/L=5	R/L=10	R/L=20	R/L=50	R/L=100	R/L=∞ (Beam)
Present	0	0.7436	0.7436	0.7436	0.7436	0.7436	0.7436
Reddy [6]		0.7332	0.7332	0.7332	0.7332	0.7332	0.7332
Present	1	0.7432	0.7431	0.7430	0.7430	0.7430	0.7430
Reddy [6]		0.7332	0.7332	0.7332	0.7332	0.7332	0.7332
Present	2	0.6832	0.6831	0.6831	0.6830	0.6830	0.6830
Reddy [6]		0.6708	0.6707	0.6707	0.6706	0.6706	0.6706
Present	5	0.6074	0.6073	0.6073	0.6072	0.6072	0.6072
Reddy [6]		0.5907	0.5906	0.5905	0.5905	0.5905	0.5905
Present	10	0.5813	0.5813	0.5812	0.5812	0.5812	0.5812
Reddy [6]		0.5770	0.5770	0.5769	0.5769	0.5769	0.5769

Table 6. Transverse shear stress for various values of length coordinate (x/L)

Theory	p	x/L=0	x/L=0.2	x/L=0.4	x/L=0.5	x/L=0.6	x/L=0.8	x/L=1
Present	0	0.7436	0.713	0.6516	0	0.6516	0.7130	0.7436
Present	1	0.7432	0.7125	0.6512	0	0.6512	0.7125	0.7432
Present	2	0.6832	0.6552	0.5991	0	0.5991	0.6552	0.6832
Present	5	0.6074	0.5828	0.5332	0	0.5332	0.5828	0.6074
Present	10	0.6619	0.6351	0.5813	0	0.5813	0.6351	0.6619

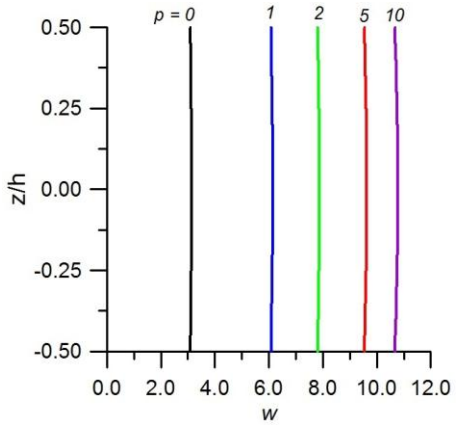

Figure 3. Variation of transverse displacement through the thickness of the arch

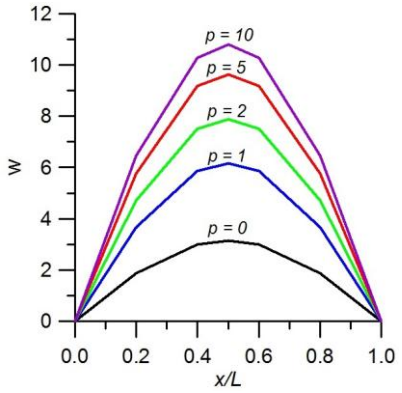

Figure 4. Variation of transverse displacement along the length of the arch

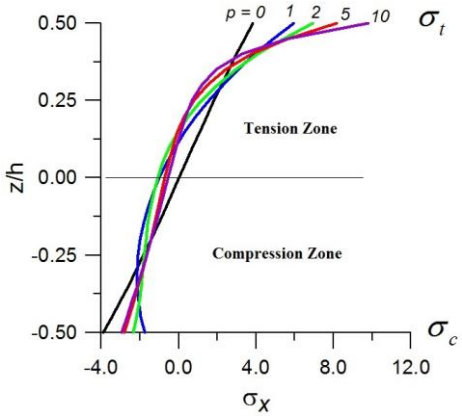

Figure 5. Variation of axial stress through the thickness of the arch

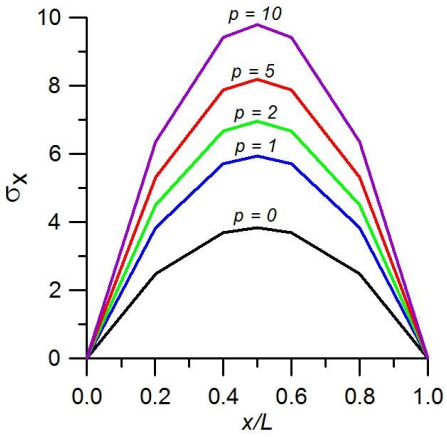

Figure 6. Variation of axial stress along the length of the arch

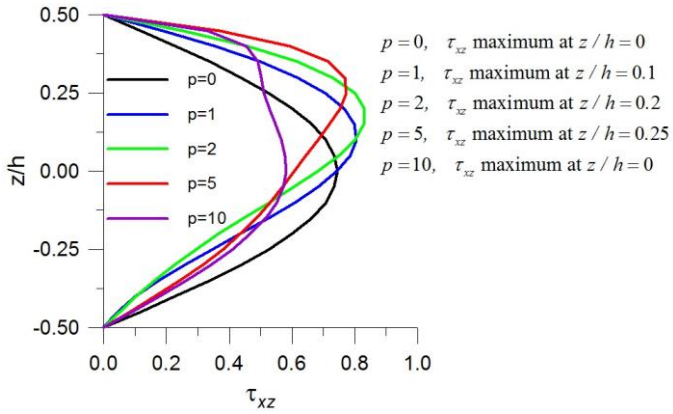

Figure 7. Variation of transverse shear stress through the thickness of the arch

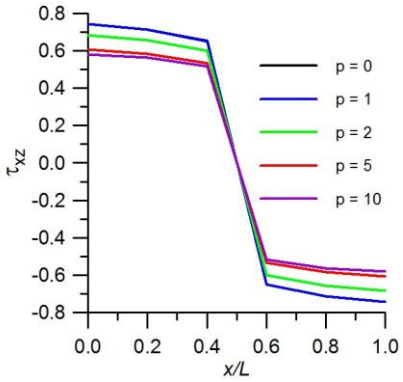

Figure 8. Variation of transverse shear stress along the length of the arch

6 CONCLUSIONS

In this paper, a trigonometric curved beam theory considering the effects of transverse shear and normal stresses is applied for the static flexural analysis of two hinge arches made up of functionally graded composite materials. The principle of virtual work is employed to derive the governing equations. The Navier's technique is used to obtain the results of the flexural analysis of simply supported FG composite arches. The effects of the power law coefficient and radius of curvature on the displacements and stresses are discussed. Based on the numerical results and discussion, it is concluded that the present theory predicts excellent results of displacement and stresses in FG composite arches subjected to uniform load. The transverse displacement increases with an increase in the power law coefficient due to the increase in flexibility. Increase in power law coefficient increases axial stress in tension zone. It is also

concluded that the increase in power law coefficient shifted the neutral axis of the arch in tension zone. Finally, it is recommended that the EBT and FSDT are not accurate to predict flexural response of thick arches made up of advanced composite materials. Therefore, for the accurate flexural analysis of advanced composite arches, it is necessary to consider the effects of both transverse shear and normal stresses.

REFERENCES

[1] Bernoulli, J, "Curvatura laminae elasticae", Acta Eruditorum Lipsiae, pp. 262 – 276, 1694.
[2] Timoshenko, SP, "On the correction for shear of the differential equation for transverse vibrations of prismatic bars", Philosophical Magazine, Vol. 41, No. 6, pp. 742-746, 1921.
[3] Sayyad, AS, Ghugal, YM, "On the free vibration analysis of laminated composite and sandwich plates: A review of recent literature with some numerical results", Composite Structures, Vol. 129, pp. 177–201, 2015.
[4] Sayyad, AS, Ghugal, YM, "Bending, buckling and free vibration of laminated composite and sandwich beams: A critical review of literature", Composite Structures, Vol. 171, pp. 486–504, 2017.
[5] Sayyad, AS, Ghugal, YM, "Modeling and analysis of functionally graded sandwich beams: A review", Mechanics of Advanced Materials and Structures, Vol. 26, No. 21, pp. 1776-1795, 2018.
[6] Reddy, JN, "A simple higher order theory for laminated composite plates", ASME Journal of Applied Mechanics, Vol. 51, pp. 745-752, 1984.
[7] Bhimaraddai, A, Carr, AJ, Moss, PJ, "Generalized finite element analysis of laminated curved beams with constant curvature", Computers and Structures, Vol. 31, No. 3, pp. 309-317, 1989.
[8] Qatu, MS, "In-plane vibration of slightly curved laminated composite beams", Journal of Sound and Vibration, Vol. 159, No. 2, pp. 327-338, 1992.
[9] Ecsedi, I, Dluhi, K, "A linear model for the static and dynamic analysis of non-homogeneous curved beams", Applied Mathematical Modelling, Vol. 29, pp. 1211–1231, 2005.
[10] Marur, SR, Kant, T, "On the flexural analysis of sandwich and composite arches through an isoparametric higher-order model", Journal of Engineering Mechanics, Vol. 135, No. 7, pp. 614-631, 2009.
[11] Guo, J, Shi, D, Wang, Q, Pang, F, Liang, Q, "A domain decomposition approach for static and dynamic analysis of composite laminated curved beam with general elastic restrains", Mechanics of Advanced Materials and Structures, Vol. 26, No. 16, pp. 1390-1402, 2018.
[12] Ye, T, Jin, G, Su, Z, "A spectral-sampling surface method for the vibration of 2-D laminated curved beams with variable curvatures and general restraints", International Journal of Mechanical Sciences, Vol. 110, pp. 170–189, 2016.
[13] Thurnherr, C, Groh, RMJ, Ermanni, P, Weaver, PM, "Higher-order beam model for stress predictions in curved beams made from anisotropic materials", International Journal of Solids and Structures, Vol. 97-98, pp. 16-28, 2016.
[14] Eroglu, U, "Large deflection analysis of planar curved beams made of functionally graded materials using variational iterational method", Composite Structures, Vol. 136, pp. 204-216, 2015.
[15] Kurtaran, H, "Large displacement static and transient analysis of functionally graded deep curved beams with generalized differential quadrature method", Composite Structures, Vol. 131, pp. 821-831, 2015.
[16] Luu, AT, Kim, N, Lee, J, "Bending and buckling of general laminated curved beams using NURBS-based isogeometric analysis", European Journal of Mechanics- A/Solids, Vol. 54, pp. 218-231, 2015.

[17] Nanda, N, Kapuria, S, "Spectral finite element for wave propagation analysis of laminated composite curved beams using classical and first order shear deformation theories", Composite Structures, Vol. 132, pp. 310–320, 2015.
[18] Hajianmaleki, M, Qatu, MS, "Static and vibration analyses of thick, generally laminated deep curved beams with different boundary conditions", Composites Part B, Vol. 43, pp. 1767–1775, 2012.
[19] Jun, L, Guangwei, R, Jin, P, Xiaobin, L, Weiguo, W, "Free vibration analysis of a laminated shallow curved beam based on trigonometric shear deformation theory", Mechanics Based Design of Structures, Vol. 42, pp. 111–129, 2014.
[20] Hajianmaleki, M, Qatu, MS, "Vibrations of straight and curved composite beams: A review", Composite Structures, Vol. 100, pp. 218–232, 2013.
[21] Nguyen, TK, Nguyen, BD, "A new higher-order shear deformation theory for static, buckling and free vibration analysis of functionally graded sandwich beams", Journal of Sandwich Structures and Materials, Vol. 17, pp. 1–19, 2015.
[22] Thai, HT, Vo, TP, "Bending and free vibration of functionally graded beams using various higher-order shear deformation beam theories", International Journal of Mechanical Sciences, Vol. 62, No. 1, pp. 57 – 66, 2012.
[23] Osofero, AI, Vo, TP, Thai, HT, "Bending behaviour of functionally graded sandwich beams using a quasi-3D hyperbolic shear deformation theory", Journal of Engineering Research, Vol. 19, No. 1, pp. 1-16, 2014.
[24] Bennai, R, Atmane, HA, Tounsi, A, "A new higher-order shear and normal deformation theory for functionally graded sandwich beams", Steel and Composite Structures, Vol. 19, No. 3, pp. 521-546, 2015.
[25] Vo, TP, Thai, HT, Nguyen, TK, Inam, F, Lee, J, "Static behaviour of functionally graded sandwich beams using a quasi-3D theory", Composites Part B, Vol. 68, pp. 59-74, 2015.
[26] Yarasca, J, Mantari, JL, Arciniega, RA, "Hermite–Lagrangian finite element formulation to study functionally graded sandwich beams", Composite Structures, Vol. 140, pp. 567–581, 2016.
[27] Sayyad, AS, Ghugal, YM, "A unified shear deformation theory for the bending of isotropic, functionally graded, laminated and sandwich beams and plates", International Journal of Applied Mechanics, Vol. 9, pp. 1-36, 2017.
[28] Sayyad, AS, Ghugal, YM, "Analytical solutions for bending, buckling, and vibration analyses of exponential functionally graded higher order beams", Asian Journal of Civil Engineering, Vol. 19, No. 5, pp. 607–623, 2018.
[29] Hebali, H, Tounsi, A, Houari, MSA, Bessaim, A, Bedia, EAA, "New quasi-3d hyperbolic shear deformation theory for the static and free vibration analysis of functionally graded plates", Journal of Engineering Mechanics, Vol. 140, No. 2, pp. 374-383, 2014.
[30] Belabed, Z, Houari, MSA, Tounsi, A, Mahmoud SR, Beg OA. An efficient and simple higher order shear and normal deformation theory for functionally graded material (FGM) plates", Composites Part B, Vol. 60, pp. 274–283, 2014.
[31] Abualnour, M, Houari, MSA, Tounsi, A, Bedia, EAA, Mahmoud, SR, "A novel quasi-3D trigonometric plate theory for free vibration analysis of advanced composite plates", Composite Structures, Vol. 184, pp. 688–697, 2018.
[32] Meziane, MAA, Abdelaziz, HH, Tounsi, A, "An efficient and simple refined theory for buckling and free vibration of exponentially graded sandwich plates under various boundary conditions", Journal of Sandwich Structures and Materials, Vol. 16, pp. 293-318, 2014.
[33] Bourada, F, Bousahla, AA, Bourada, M, Azzaz, A, Zinata, A, Tounsi, A, "Dynamic investigation of porous functionally graded beam using a sinusoidal shear deformation theory", Wind and Structures, An International Journal, Vol. 28, No. 1, pp. 19-30, 2019.
[34] Bourada, M, Kaci, A, Houari, MSA, Tounsi, A, A new simple shear and normal deformations theory for functionally graded beams. Steel Composite Structures, Vol. 18, No. 2, pp. 409-423, 2015.

[35] Zemri, A, Houari, MSA, Bousahla, AA, Tounsi, A, "A mechanical response of functionally graded nanoscale beam: an assessment of a refined nonlocal shear deformation theory beam theory", Structural Engineering and Mechanics, Vol. 54, No. 4, pp. 693-710, 2015.
[36] Sayyad, AS, Ghugal, YM, "An inverse hyperbolic theory for FG beams resting on Winkler-Pasternak elastic foundation", Advances in Aircraft and Spacecraft Science, An International Journal, Vol. 5, No. 6, pp. 671-689, 2018.
[37] Tornabene, F, "Free vibration analysis of functionally graded conical, cylindrical shell and annular plate structures with a four-parameter power-law distribution", Computer Methods in Applied Mechanics and Engineering, Vol. 198, pp. 2911–2935, 2009.
[38] Tornabene, F, Liverani, A, Caligiana, G, "FGM and laminated doubly curved shells and panels of revolution with a free-form meridian: A2-DGDQ solution for free vibrations", International Journal of Mechanical Sciences, Vol. 53, pp. 446–470, 2011.
[39] Tornabene, F, Fantuzzi, N, Bacciocchi, M, Viola, E, "Effect of agglomeration on the natural frequencies of functionally graded carbon nanotube-reinforced laminated composite doubly curved shells", Composites Part B, Vol. 89, pp. 187-218, 2016.
[40] Tornabene, F, Reddy, JN, "FGM and laminated doubly-curved and degenerate shells resting on nonlinear elastic foundations: A GDQ solution for static analysis with a posteriori stress and strain recovery", Journal of the Indian Institute of Science, Vol. 93, No. 4, pp. 635-688, 2013.
[41] Tornabene, F, Fantuzzi, N, Viola, E, Batra, RC, "Stress and strain recovery for functionally graded free-form and doubly-curved sandwich shells using higher-order equivalent single layer theory", Composite Structures, Vol. 119, pp. 67–89, 2015.
[42] Sayyad, AS, Ghugal, YM, "Static and free vibration analysis of laminated composite and sandwich spherical shells using a generalized higher-order shell theory", Composite Structures, Vol. 219, pp. 129–146, 2019.